Vortex merging, oscillation, and quasiperiodic structure in a linear array of elongated vortices

Hiroaki Fukuta[1] and Youichi Murakami[2]
[1]*Department of Mathematical Sciences, College of Engineering, Osaka Prefecture University, Sakai 599, Japan*
[2]*Department of Aerospace Engineering, College of Engineering, Osaka Prefecture University, Sakai 599, Japan*
(Received 27 November 1996)

Linear stability and the secondary flow pattern of the rectangular cell flow, $\Psi = \sin kx \sin y$ $(0<k<\infty)$, are investigated in an infinitely long array of the x direction $[(-\infty,\infty)\times[0,\pi]]$ or various finite M arrays $([0,M\pi/k]\times[0,\pi])$ on the assumption of a stress-free boundary condition on the lateral walls. The numerical results of the eigenvalue problems on the infinite array show that a mode representing a global circulating vortex in the whole region ($\psi \approx \sin y$) appears in the y-elongated cases ($k>1$), which confirm the secondary flow observed in Tabeling *et al.* [J. Fluid Mech. **213**, 511 (1990)], while a mode representing *quasiperiodic* arrays of counter-rotating vortices appears in the x-elongated cases ($k<1$) at large critical Reynolds number. In large finite arrays the mode connected with those of the case $M=\infty$ appears for most cases while another (oscillatory) mode appears for vortices elongated in the y direction. The parameter region of the oscillatory modes becomes wider when the system size (M) becomes smaller. For a pair of counter-rotating vortices ($M=2$) at the point k_0 between the regions of the two modes the critical Reynolds number takes an extreme large value. Analysis of a finite nonlinear system obtained by the Galerkin method shows the nonlinear saturation of the critical modes, though its results are in quantitative agreement with those of the linear stability in a limited region of k. [S1063-651X(97)12905-1]

PACS number(s): 47.54.+r, 47.20.−k, 47.32.−y

I. INTRODUCTION

Research on pattern formation in a nonequilibrium dissipative system is regarded as a fundamental problem in modern physics. One of the simplest nontrivial spatial patterns is apparently a periodic structure. This structure appears generic in the sense that it is formed through the nonlinear saturation of the unstable mode to a quiescent state. The bifurcation of the periodic structure is a central topic of the pattern formation in nonequilibrium systems such as fluid dynamics, chemical reaction systems, and so on. Various kinds of instability from the periodic structures, especially so-called rolls, are found and analyzed based on the basic equations and the reduced equations such as the envelope equation, the phase equation, and so on [1–3].

Here we consider the problem of the stability and the bifurcation of a linear array of counter-rotating vortices in a very thin layer of incompressible viscous fluids. The basic state has a one-dimensional periodicity in an infinitely extended array. In laboratory experiments equipment is devised to realize such spatially periodic flows in which an electrolyte or a liquid metal in a very shallow vessel is driven by the action of Lorentz force periodically arranged. Such experiments are now widely performed by several groups [4–7] to investigate the bifurcation of the flows and the two-dimensional turbulence. In particular, an initial stage of our investigation [8], where two-dimensional unbounded lattices of vortices are considered, aims to explain the results of the experiments by Tabeling *et al.* [6] theoretically. Here we clarify the nature of its stability, thoroughly taking into account the lateral boundaries and the wide range of parameters. It is known that this type of flow is approximately described by the two-dimensional Navier-Stokes equation with inhomogeneous terms due to an external forcing and additional damping terms originating from the bottom friction, although a suitable representation of the frictional effect is still being debated [4,9]. Along this line, we adopt the two-dimensional Navier-Stokes equation in order to analyze our problem.

In the Rayleigh-Bénard problem and the Taylor-Couette problem, which are regarded as a paradigm of the pattern-forming hydrodynamical systems, periodic structures emerge spontaneously by a linearly unstable mode, not by an external forcing; the form of the observed vortices is almost isotropic. On the other hand, in our problem the form and the configuration of the vortices are controlled by the applied forcing and the setup of the experimental apparatus with relative ease. Actually the linear array of the elongated vortices is achieved in the experiment by Tabeling *et al.* [6]. Hence this problem is very suitable to investigate how the structure of the individual vortex in the linear array correlates with the type of bifurcation or the dominant linearly unstable mode. In this study we focus on the structure of the unstable mode of several arrays of various elongated vortices in this paper. Here we do not consider more general configurations, or lattices of vortices. The linear stability of square lattices of isotropic vortices was investigated by Thess [10], who did not consider the case of the linear array. The results were extended to arbitrary lattices of the isotropic vortices in Fukuta and Murakami [11], where a qualitative difference between the linear array and the others was discussed.

In addition to the above purpose, the interaction of several concentrated vortices is a fundamental problem in fluid dynamics. A part of our problem seems related to the dynamics of separated vortices in a wall of confined systems which often appear in engineering applications. For example, in rapidly diverging channel flow a pair of counter-rotating vortices appears attached to the diverging part of the wall [12]. This situation is achieved approximately planar; it resembles the case of a pair of counter-rotating vortices in a rectangular

region treated here. Therefore it is expected that our problem is useful to understand a general feature of the stability of the planar vortices confined by the rigid wall. The roll observed in the convection of the troposphere is often stretched horizontally [13]. Our results of long arrays of the vortices may give some insight into the secondary bifurcation of this pattern.

This paper is organized as follows. First, we present the main flow modeling the elongated vortex, formulate the problem of the linear stability, and state the assumption of our treatment. Second, we give the main results of the linear stability, i.e., the critical Reynolds number and the structure of the critical mode. Third, in order to investigate qualitative nonlinear dynamics we introduce and analyze the system of the limited modes on the basis of the Galerkin method. Finally, we summarize our results, discuss the relation of the experiments and other problems, and comment on possible future works.

II. FORMULATION OF THE PROBLEM

We consider a linear array in the x direction of the rectangular vortices represented by

$$\overline{\Psi}(x,y)=\sin kx\ \sin y, \tag{1}$$

where $0<k<\infty$. Hence this flow neglects the inner structure of the individual vortex observed in experiments, though its streamlines resemble the observed ones. The reason for choosing this flow is to conduct the eigenvalue problem relatively easily in numerical computation. We consider two types of regions:

$$D_{M,1}=[0,M\pi/k]\times[0,\pi], \tag{2}$$

$$D_{\infty,1}=(-\infty,\infty)\times[0,\pi]. \tag{3}$$

Note that the main flow does not satisfy the nonslip (viscous) boundary condition (or rigid boundary condition), only the impermeable condition. In addition to the latter, the relation $\Delta\Psi=0$ holds; the so-called stress-free boundary condition is satisfied. These conditions may not be satisfied well in side walls of laboratory experiments. Nevertheless, we accept the assumption because the numerical calculation is much easier than the nonslip condition. The justification for this assumption requires comparison with experiments or numerical calculation with the nonslip condition. Later we argue this point in Concluding Remarks.

Since the flow is realized in a very thin layer, we consider the governing equation for two-dimensional incompressible fluids as follows:

$$\frac{\partial\Delta\Psi}{\partial t}+\frac{\partial(\Delta\Psi,\Psi)}{\partial(x,y)}=\frac{1}{R}\Delta^2\Psi-\frac{(k^2+1)^2}{R}\sin kx\ \sin y, \tag{4}$$

where all quantities have been made nondimensional, t is the time, Ψ is a stream function, R is the Reynolds number, $\Delta f=(\partial^2 f/\partial x^2)+(\partial^2 f/\partial y^2)$, and $\partial(f,g)/\partial(x,y)=(\partial f/\partial x)(\partial g/\partial y)-(\partial f/\partial y)(\partial g/\partial x)$. The last inhomogeneous term represents an external force, which permits the main flow to exist. Here we neglect the effect of the bottom friction that inevitably exists in laboratory experiments. This is also a strong assumption for our treatment. Therefore we would like to stress that our treatment should be regarded as a *model* in connection with the laboratory experiments.

The linearized equation governing the stream function $\psi(x,y,t)$ of infinitesimal disturbance superposed on the main flow (1) is given by

$$\frac{\partial\Delta\psi}{\partial t}+\frac{\partial(\Delta\overline{\Psi},\psi)}{\partial(x,y)}+\frac{\partial(\Delta\psi,\overline{\Psi})}{\partial(x,y)}=\frac{1}{R}\Delta^2\psi, \tag{5}$$

where we omit the nonlinear term of the disturbances. We also apply the stress-free boundary conditions for the disturbance:

$$\psi=\Delta\psi=0, \tag{6}$$

which is the same as that of the main flow. In accordance with Eq. (6), the stream function in the finite array, $D_{M,1}=[0,M\pi/k]\times[0,\pi]$, is expanded as

$$\psi(x,y,t)=\exp(\sigma t)\sum_{m,n=1}^{\infty}a_{m,n}\sin\frac{m}{M}x\ \sin ny. \tag{7}$$

Note that the application of the stress-free boundary condition as a substitute for a viscous boundary condition means replacement of the first derivative of the stream function with the second one. Hence the number of boundary conditions is suitable for the viscous term. We also expand the stream function in the infinitely long array, $D_{\infty,1}=(-\infty,\infty)\times[0,\pi]$, as

$$\psi(x,y,t)=\exp(\sigma t+i\alpha x)\sum_{m=1}^{\infty}a_m\sin ny, \tag{8}$$

where $\alpha(0<\alpha<1)$ is a real Floquet number.

Substitution of Eqs. (7) and (8) into Eq. (5) leads to an infinite set of simultaneous algebraic equations for $a_{m,n}$ expressed symbolically as $\sigma a=Da$, where a and D are the two- and four-dimensional matrices of infinite order, respectively. Therefore we can obtain the growth rate $\sigma_r=\mathrm{Re}[\sigma]$ by solving this eigenvalue problem. We reduce the range of exponents to $0<\alpha<0.5$ due to the form of the main flow (1). In the numerical computation we replace the infinite set with a finite set of equations ($|m|\leqslant N_x, |n|\leqslant N_y$). In order to get sufficient accuracy, $N_x\times N_y$ should be varied in a wide range between 3×4 and 8×40.

In an unbounded region, $(-\infty,\infty)\times(-\infty,\infty)$, the solution of Eq. (5) is represented in the form

$$\tilde{\psi}_{\alpha,\beta}(x,y,t)=\exp[\tilde{\sigma}t+i(\alpha kx+\beta y)]F_{\alpha,\beta}(kx,y), \tag{9}$$

since the coefficient functions in Eq. (5) have the period $2\pi/k$ in x and 2π in y, where α and β are (real) Floquet exponents. The symmetry of the main flow $\Psi(-x,y)=\Psi(x,-y)=-\Psi(x,y)$ ensures that linear combinations

$$\tilde{\psi}_{\alpha,\beta}(x,y,t)-\tilde{\psi}_{\alpha,\beta}(-x,y,t)-\tilde{\psi}_{\alpha,\beta}(x,-y,t)+\tilde{\psi}_{\alpha,\beta}(-x,-y,t)$$

and

$$\tilde{\psi}_{\alpha,\beta}(x,y,t)-\tilde{\psi}_{\alpha,\beta}(x,-y,t)$$

are also a solution of Eq. (9) in an unbounded region. The former combination of $\tilde{\psi}_{\alpha,\beta}$ satisfies the boundary condition (6) in $D_{M,1}$ for some discrete values of α_m,β_n:

$$\alpha_m=\frac{m}{M},\quad \beta_n=0,\quad \left(m=0,\ldots,\left[\frac{M}{2}\right]\right), \tag{10}$$

where $[x]$ denotes the largest natural number that is not greater than x. The eigenmode $\tilde{\psi}$ is represented by

$$\psi(x,y,t)=\tilde{\psi}_{\alpha_m,\beta_n}(x,y,t)-\tilde{\psi}_{\alpha_m,\beta_n}(-x,y,t)-\tilde{\psi}_{\alpha_m,\beta_n}(x,-y,t)+\tilde{\psi}_{\alpha_m,\beta_n}(-x,-y,t), \tag{11}$$

In a similar way we have the representation for $D_{\infty,1}$,

$$\psi(x,y,t)=\tilde{\psi}_{\alpha,\beta_n}(x,y,t)-\tilde{\psi}_{\alpha,\beta_n}(x,-y,t). \tag{12}$$

In order to save the CPU time we often use the results of the linear stability in an unbounded region and relate them to the problem $D_{M,1}$ instead of solving the problem directly.

III. RESULTS OF LINEAR STABILITY

In this section we give the results of the linear eigenvalue problem. We have two parameters characterizing the main flows: $1/k$ is the ratio of the length of the sides of each vortex and M is the number of the vortices. Hereafter we use $1/k$ instead of k for convenience. Hence the case with small $1/k$ corresponds to the y-elongated vortex while that with large $1/k$ to the x-elongated vortex.

A. Infinitely large array of vortices: $M=\infty$

Here we neglect the lateral boundaries that are parallel to the y axis; it is the simplest case of all and has the same symmetry of the roll in the infinite region. We present the main results of the critical Reynolds number for various values of the inverse of the parameter $1/k$ between 0 and 1.2 in Fig. 1. This shows that the critical Reynolds number increases with increasing $1/k$. The curve in the range $0<1/k<1$ is the same as the Reynolds number due to the *periodic mode* in Fig. 1 of [8]. Note that k in that work corresponds to $1/k$ in this work. The large-scale mode, which has an almost uniform structure and whose growth rate shows the negative eddy viscosity, is excluded by the lateral boundaries. We would like to stress that the array of the y-elongated vortices $(1/k<1)$ becomes unstable at relatively low Reynolds number while that of the x-elongated vortices $(1/k>1)$ becomes remarkably stable. We do not obtain the critical Reynolds number for $1/k>1.2$ because of the lack of memory of the standard workstation. This result suggests that the ratio of the sides k is a very important factor on the order of the critical Reynolds number.

Next we describe the character of the critical modes. The critical modes are always *stationary* (i.e., Im $\sigma=0$); the bifurcation is expected to be a pitchfork type and cause a transition from a stable steady state to one of the two steady

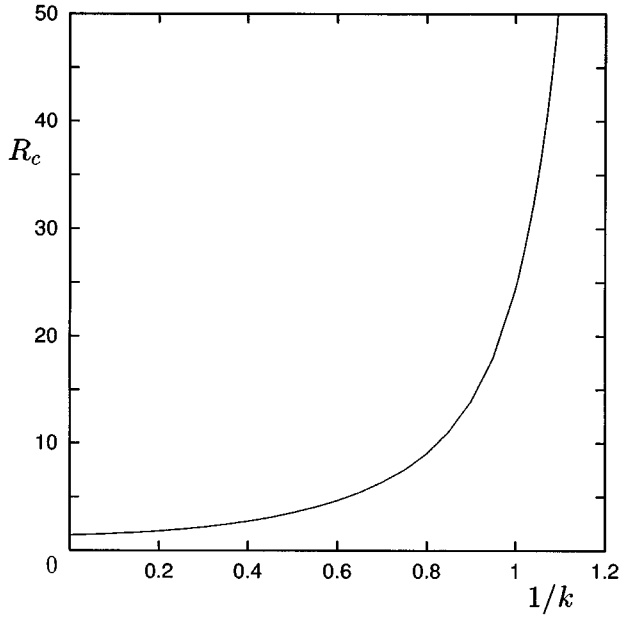

FIG. 1. The critical Reynolds number R_c in the range $0<1/k<1.2$ for $M=\infty$.

branches of an intersecting parabolic curve at the critical Reynolds number. In the next section we will discuss the nature of the bifurcation based on a crude Galerkin approximation. The Floquet exponent α_c of the critical modes is always zero for $0<1/k<1$ while α_c is nonzero for $1/k>1$. Figure 2 shows that α_c grows abruptly in the range $1/k>1$ and takes a value of 0.5 at $k=1.16$. Note that α is less than 0.5 for the symmetry. Figure 3 shows how the marginal Reynolds numbers depend on α for several $1/k$. The Reynolds number at the origin changes from minimum to maximum. At $k=1$ the second derivative of $R(k,\alpha=0)$ vanishes. The modes should be regarded as a modulation of the periodic

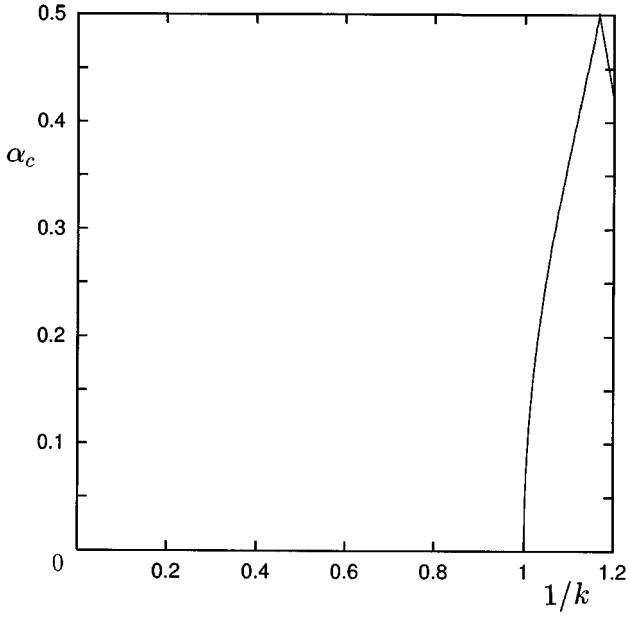

FIG. 2. The critical Floquet exponent α_c in the range $0<1/k<1.2$ for $M=\infty$.

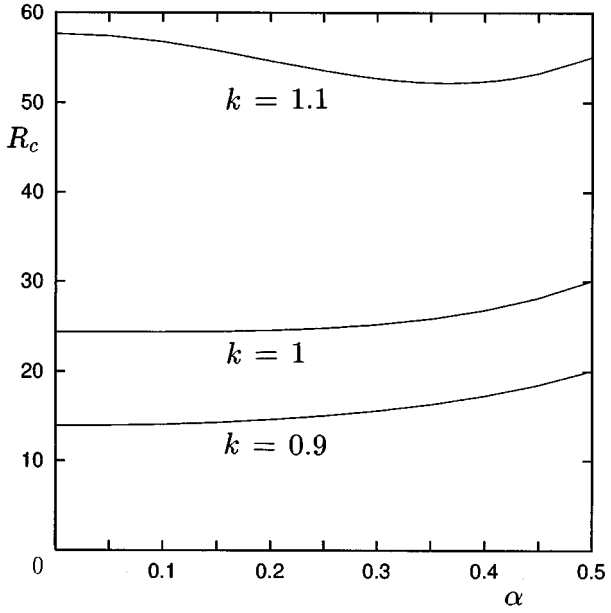

FIG. 3. The marginal Reynolds number $R(\alpha)$ for $k=0.9,1,1.1$ for $M=\infty$.

mode at $\alpha=0$ with the part $\exp(i\alpha x)$. Generally the periodicity $2\pi/\alpha$ is incommensurate with the basic periodicity; we call these types of modes *quasiperiodic* modes.

Figure 4(a) shows the structure of the periodic mode for $k=0.33$, which shows the global rotation similar to the case $k=1$ [11]. In the upper part the flow is directed rightward while it is directed leftward in the lower part. As was pointed out [8], the streamlines of the superposition of the main flow and the disturbance in Fig. 4(b) are very similar to the ones observed by the experiments [6]. The linear array becomes composed of tilted vortices, alternatively big and small. As the disturbance grows, half the vortices are expanding and

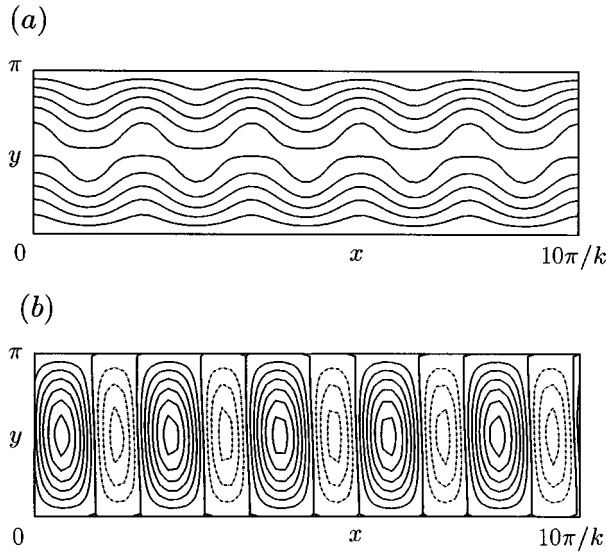

FIG. 4. (a) The streamlines of the critical mode of $k=0.33$. (b) The streamlines of $\Psi=\sin kx\,\sin y+c\psi$ (c is 0.3, ψ is the *periodic* mode, and $|\psi|_{\max}=1$) in the case with $k=0.33$.

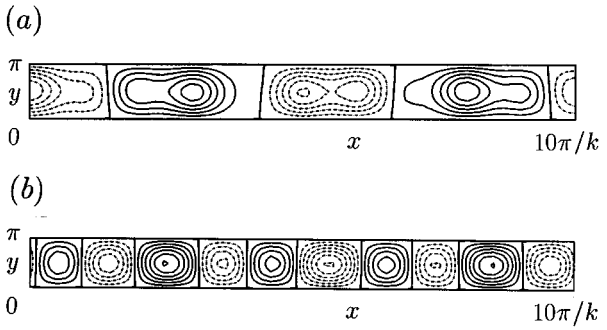

FIG. 5. (a) The streamlines of the critical mode of $k=1.1$. (b) The streamlines of $\Psi=\sin kx\,\sin y+c\psi$ (c is 0.3, ψ is the *quasiperiodic* mode, and $|\psi|_{\max}=1$) in the case with $k=0.33$.

the others are squeezing. The growing process of the disturbance looks like *vortex merging* of pairs of counter-rotating vortices. It should be noted that this merging is qualitatively different from the merging of the vortex with the same sign of vorticity usually observed in an unbounded region. As usual in pitchfork bifurcation, the sign of the vorticity is not determined by the theory of the ideal situation; some biases in the laboratory experiments may play a decisive role in its selection. Figure 5(a) shows the structure of the critical mode for $k=1.1$, which shows the stationary *quasiperiodic* structure. The change of the sign of the vorticity is due to the part of the exponential factor of the eigenmode [i.e., $\exp(i\alpha x)$]. It is confirmed that the structure of the periodic part, $F(kx,y)$, is similar to that of the periodic mode. Superposition of the main flow and the mode shows the quasiperiodic array of the vortices in Fig. 5(b). This is, to our knowledge, the first theoretical evidence of spontaneous formation of a quasiperiodic chain of vortices from the periodic chain, though the laboratory experiments in these cases have not been performed yet. Note that the large critical Reynolds number corresponds to the appearance of a quasiperiodic mode.

B. A pair of vortices: $M=2$

In contrast with Sec. III A, we consider another limit i.e., the smallest systems of the counter-rotating vortices. We note that no experiments of this configuration have been conducted yet, though the transition from two pairs of counter-rotating systems is investigated in the experiments of Tabeling *et al.* [6].

We present the main results of the critical Reynolds number for various values of the inverse of the parameter $1/k$ between 0 and 1.2 in Fig. 6. There are two critical curves in contrast with the preceding subsection. The critical Reynolds number for a given k is always larger than the corresponding one for the infinitely long array. This is a natural result because the confinement of the system excludes the large-scale disturbances. A stationary mode gives the right curve while another oscillatory mode gives the left one. It is a remarkable fact that R_c becomes very large around $k=0.5$, though we do not obtain an accurate value. Apart from this region, the tendency of the right curve resembles that of the curve in Fig. 1. This result also suggests that the ratio of the sides, k, is a very important factor on the order of the critical Reynolds number.

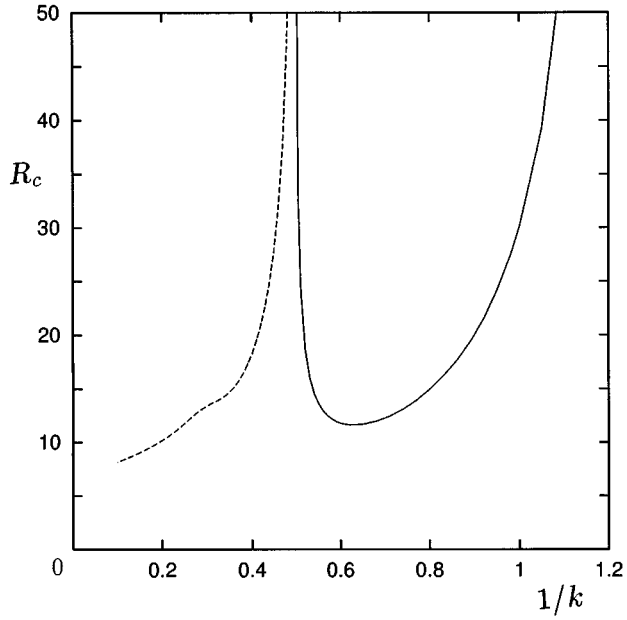

FIG. 6. The critical Reynolds number R_c in the range $0<1/k<1.2$ for $M=2$. The bold line is due to the stationary mode; the dashed line is due to the oscillatory mode.

Next we describe the character of the critical modes. The critical modes are *stationary* (i.e., Im $\sigma=0$) in the range $1/k>0.5$; the bifurcation is expected to be a pitchfork. On the other hand, the modes are *oscillatory* (i.e., Im $\sigma\neq0$) in the range $1/k<0.5$; the Hopf bifurcation is expected. The frequency of the critical modes decreases with $1/k$ increasing until $1/k=0.5$, as shown in Fig. 7. In the next section we will discuss the nature of the bifurcation based on a crude Galerkin approximation.

Figure 8(a) shows the structure of the stationary mode for $k=0.6$, which shows the global rotation of a system size.

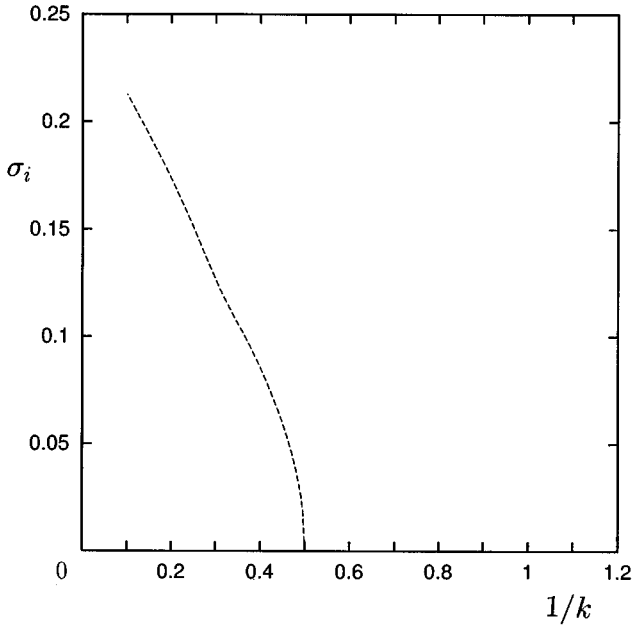

FIG. 7. The critical frequency σ_{ic} in the range $0<1/k<1.2$ for $M=2$.

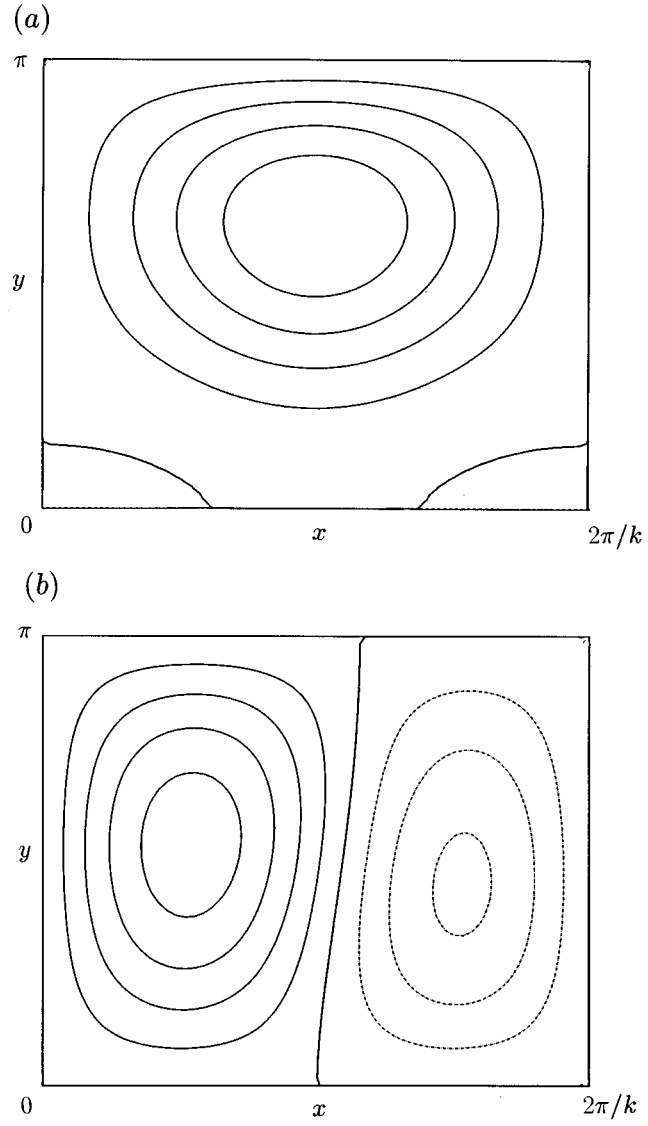

FIG. 8. (a) The streamlines of the critical mode of $k=1.1$. (b) The streamlines of $\Psi=\sin kx\,\sin y+c\psi$ (c is 0.3, ψ is the *stationary* mode, and $|\psi|_{\max}=1$) in the case with $k=0.6$.

The streamlines are symmetric with $x=\pi/k$. However, the velocity does not have a reflectional symmetry with $x=\pi/k$ as opposed to the main flow. As usual in pitchfork bifurcation, the sign of the vorticity is not determined by the theory. Figure 8(b) shows that one vortex is expanding and the other is shrinking as the disturbance is growing. It also looks like a vortex merging of a pair of counter-rotating vortices. Figures 9(a) and 9(b) show one-quarter of the period of the oscillation of the structure of the critical mode for $k=0.4$. At an initial time with a suitable phase [Fig. 9(a)] it looks like a global rotation of the stationary mode. At one-quarter of the period it looks a pair of counter-rotating vortices. The separated streamline is nearly parallel to the x axis; it is approximately normal to that of the main flow. Figures 9(c) and 9(d) show that the flow of the main flow plus the mode has no apparent symmetry; it becomes less symmetric than the main flow.

This type of oscillation is observed in the four-vortex system [14]. In this problem the interchange of the modes simi-

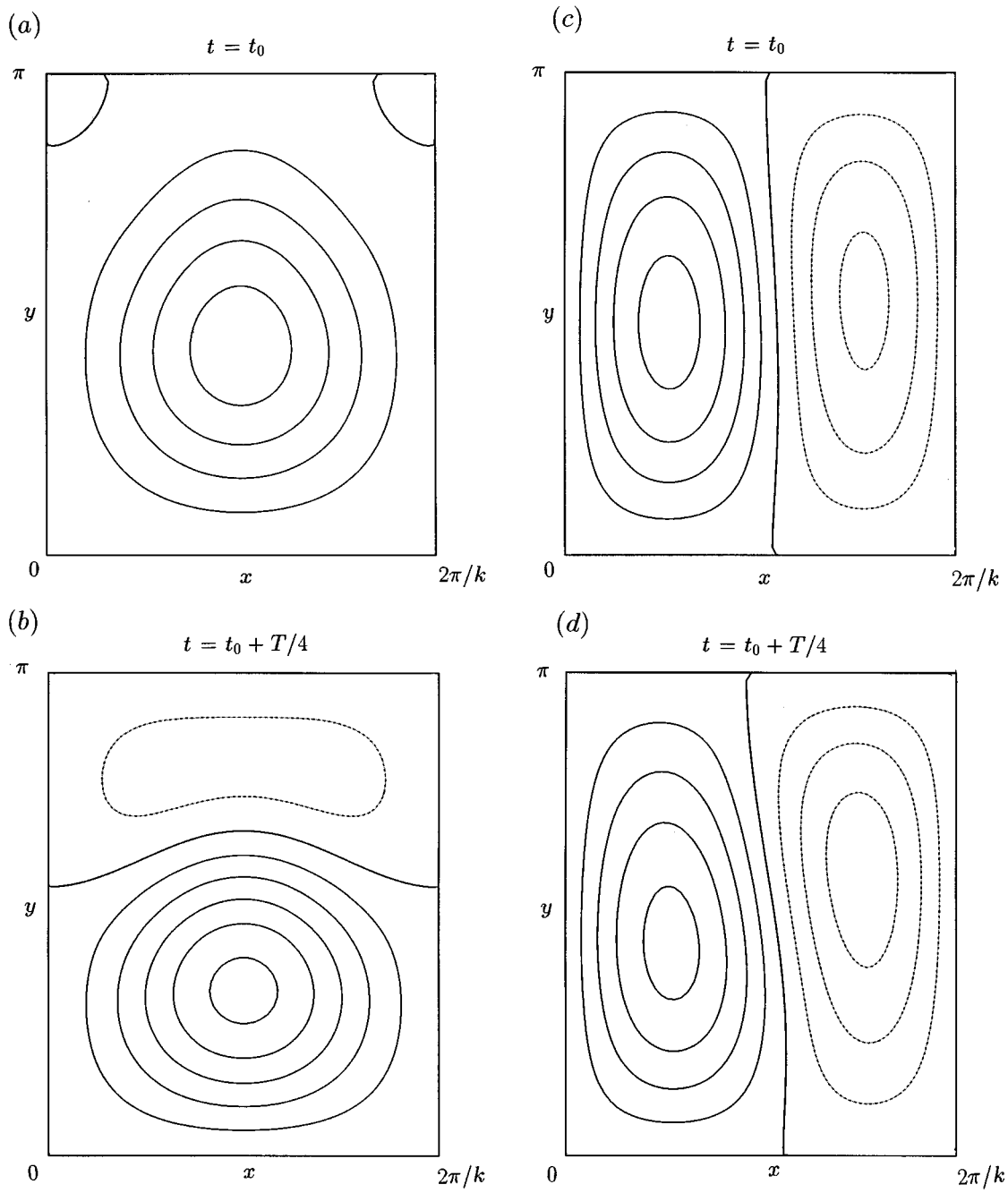

FIG. 9. (a) The streamlines of the critical mode of $k=0.4$ at $t=t_0$. (b) The same as (a) at $t=t_0+T/4$. (c) The streamlines of $\Psi = \sin kx \sin y + c\psi$ (c is 0.3, ψ is the *oscillatory* mode, and $|\psi|_{\max}=1$) in the case with $k=0.4$ at $t=t_0$. (d) The same as (d) at $t=t_0+T/4$.

lar to our problem is shown by the analysis of the truncated system and a few laboratory experiments. Hence the oscillatory instability may be generic in the interaction of the y-elongated vortices in a strongly confined system. However, the singular behavior similar to our problem is not obtained in the four-vortex system.

C. Medium size of arrays of vortices: $M=3,4$

A natural question arises: how are the above two extreme cases connected?

Figure 10 shows the results of the critical Reynolds number of three vortices: $M=3$ with the cases $M=2$ and $M=\infty$. Three curves are found. The right one (closed triangles) represents the stationary mode, which behaves in a way similar to the stationary mode of $M=2$. It is between the curves of $M=2$ and $M=\infty$ as we expect. The position of the extreme large value of the critical Reynolds number shifts leftward. The middle curve (open triangles) represents the oscillatory mode, which crosses the right curve in contrast with the case $M=2$. The left curve (closed triangles) represents another stationary mode, which does not appear in case $M=2$. Figure 11 shows the results of the critical Reynolds number of two pairs of vortices: $M=4$ with the cases $M=2$ and $M=\infty$, which is similar to Fig. 10 qualitatively.

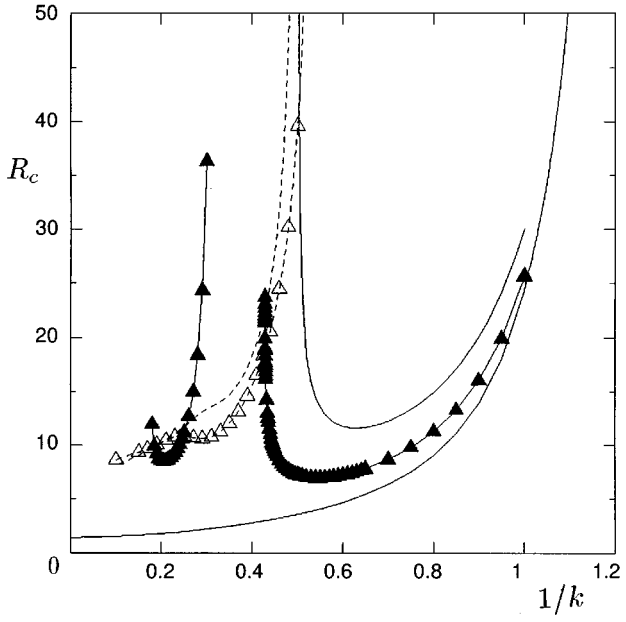

FIG. 10. The critical Reynolds number R_c in the range $0<1/k<1.2$ for $M=3$. Lower bold line, the stationary mode for $M=\infty$; upper bold line, the stationary mode for $M=2$; dashed line, the oscillatory mode for $M=2$; closed triangles, the stationary mode for $M=3$; open triangles, the oscillatory mode for $M=3$.

From Figs. 10 and 11 we learn that the results for relatively large $1/k(>0.5)$ are not changed appreciably for various M. On the other hand, a little complicated interchange of the modes is observed in the range $1/k<0.5$. Here we do not pursue the details of the region $1/k<0.1$.

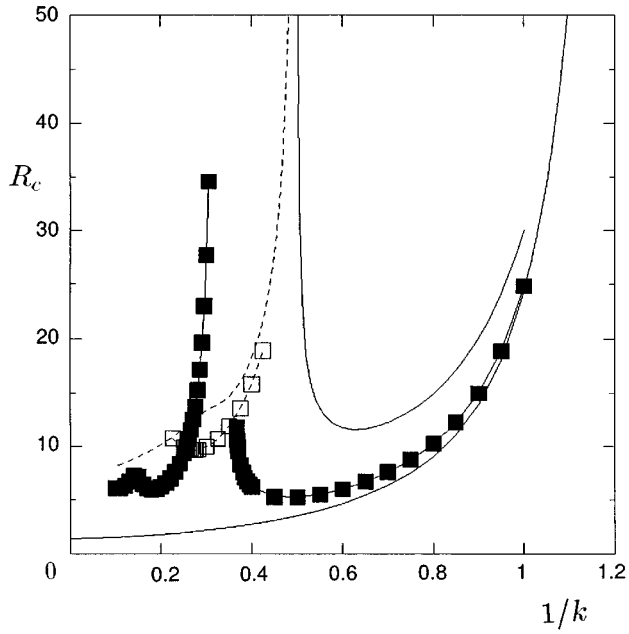

FIG. 11. The critical Reynolds number R_c in the range $0<1/k<1.2$ for $M=3$. Lower bold line, the stationary mode for $M=\infty$; upper bold line, the stationary mode for $M=2$; dashed line, the oscillatory mode for $M=2$; closed squares, the stationary mode for $M=4$; open squares, the oscillatory mode for $M=4$.

IV. RESULTS OF NONLINEAR TRUNCATED SYSTEMS

In this section we clarify a nonlinear development of the disturbance and a formation of the secondary flow pattern using a severely truncated system based on the Galerkin method. It is expected that the cases with small critical Reynolds number are explained reasonably because the truncation number $N_x \times N_y$ is small enough to obtain a reliable critical number.

A. Infinitely large array of vortices: M=∞

The principle of the truncation is based on the results of the eigenvalue problem in the preceding section. In our problem the structure of the eigenmode includes the largest component, which is limited by the system size. Usually it corresponds to the most energy-containing component. Hence we must include at least the main flow and the largest component in the truncated system. Nonlinear interaction between modes produces other modes. Furthermore, these modes interact with the former two modes so as to generate other modes. Here we only take the former two modes and the modes produced by them and construct the nonlinear ordinary differential system. Hence it is regarded as the *minimum* nonlinear truncated system.

Based on this principle we expand the stream function as follows:

$$\Psi(x,y,t)=\psi_0(t)\sin kx\ \sin y+\psi_1(t)\sin y + \psi_2(t)\cos kx\ \sin 2y. \tag{13}$$

The first term is the main flow, the second term is the largest Fourier component in the linear eigenmode. These terms generate the last term through the nonlinear interaction.

Substitution of Eq. (13) into the basic equation (4) gives the coupled ordinary differential equations as follows:

$$\frac{d\psi_0}{dt}=\frac{k(k^2+3)}{2(k^2+1)}\,\psi_1\psi_2-\frac{k^2+1}{R}\,\psi_0+\frac{(k^2+1)F}{R},$$

$$\frac{d\psi_1}{dt}=-\frac{3k}{4}\,\psi_2\psi_0-\frac{1}{R}\,\psi_1,$$

$$\frac{d\psi_2}{dt}=-\frac{k^3}{2(k^2+4)}\,\psi_0\psi_1-\frac{k^2+4}{R}\,\psi_2. \tag{14}$$

Note that we replace the forcing term by $-[(k^2+1)^2F/R]\sin kx\sin y$ in Eq. (4).

Next we set the left-hand side of Eq. (15) equal to zero in order to obtain the fixed point (or the steady state). Two types of fixed points are found:

$$\overline{\psi_{p0}}=F,$$

$$\overline{\psi_{p1}}=0,$$

$$\overline{\psi_{p2}}=0, \tag{15}$$

which represents the main flow maintained by the external forcing without disturbances. No existence condition is required as we expect,

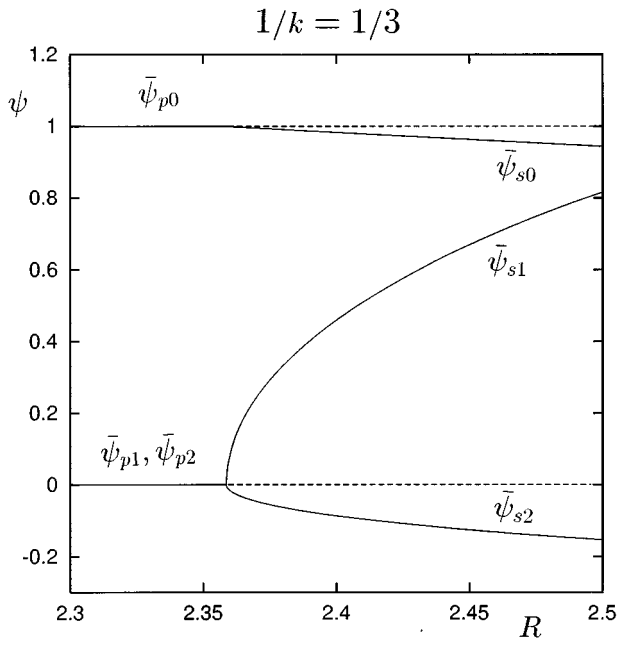

FIG. 12. The steady state is plotted at $F=1$. The critical Reynolds number is 2.36.

$$\overline{\psi_{s0}}=\frac{2\sqrt{6}}{3}\frac{k^2+4}{k^2}\frac{1}{R},$$

$$\overline{\psi_{s1}}=\pm\frac{2}{R}\frac{(k^2+1)(k^2+4)}{k^2\sqrt{k^2+3}}\left(\frac{F}{\psi_0}-1\right)^{1/2},$$

$$\overline{\psi_{s2}}=-\frac{\sqrt{6}}{3}\frac{k}{k^2+4}\psi_1, \tag{16}$$

which represents the secondary steady flow with saturated disturbances. The latter exists only if the following inequality is satisfied:

$$\frac{F}{\psi_0}-1>0, \tag{17}$$

which is also written as

$$F>\frac{2\sqrt{6}}{3R}\frac{k^2+4}{k^2}. \tag{18}$$

It is remarkable that the component of the main flow ψ_0 is constant irrespective of F in Eq. (15) if we fix R and increase F. Hence the excess energy is used only to make the disturbance grow. This feature is illustrated in Fig. 12. The results are essentially the same as those of the three-wave resonance with constant forcing and damping [15]. In Fig. 12 we fix F $(=1)$ and increase R in order to compare the results of the linear eigenvalue problem.

The linear stability of the former fixed point gives the critical condition

$$R_c=\frac{2\sqrt{6}}{3F}\frac{k^2+4}{k^2}. \tag{19}$$

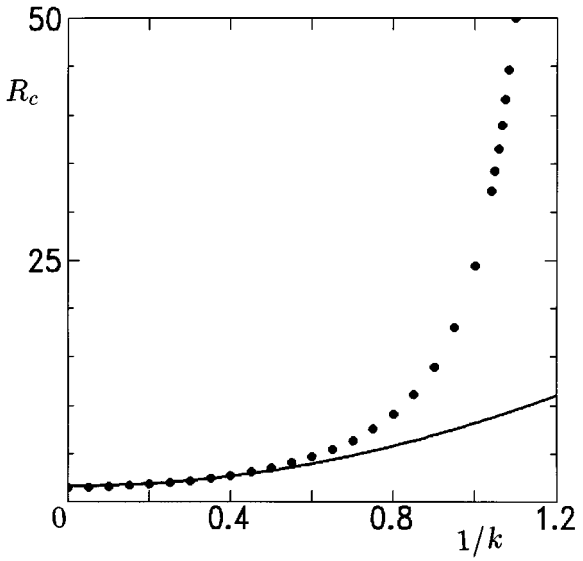

FIG. 13. The critical Reynolds number R_c in the range $0<1/k<1.2$ for $M=\infty$. The bold line is by the three-mode truncated system; the closed circles are by the converged value of the eigenvalue problems.

This corresponds to the existence condition of the latter fixed points, though we fix the forcing constant F here. The unstable mode for the fixed point has no imaginary part. Numerical simulation of the truncated system shows that the unstable mode to the main flow, ψ_p, grows to saturate and constitutes the secondary steady flow ψ_s. Hence this bifurcation is a *normal* pitchfork. From Fig. 13 the critical value R_c grows with increasing $1/k$, which is consistent with the results of the eigenvalue problem. The agreement between them for $1/k<0.5$ is remarkable.

According to the linear stability, the latter fixed point is always stable for arbitrary R and F if they are satisfied with the existence condition (18). A number of numerical simulations of the system (15) always show that the fixed point is globally stable, though we do not prove the global stability of the latter fixed point rigorously. Note that the former fixed point is shown to be globally stable when it is linearly stable [15]. Hence we cannot predict the secondary instability in the framework of this system. Indeed this does not mean that the secondary instability never occurs in the originally treated problem. An increase of the truncation number may cause the results to change qualitatively. However, our major concern is to understand the primary instability of the main flow; this problem is beyond our scope.

In Fig. 14 we plot the ratio of the component generated through the nonlinear interaction to the most energy-containing mode: $|\psi_2|/|\psi_1|$. The solid line shows the results of the steady state (the latter fixed point) in the truncated system while the open circles are obtained by the linear eigenvalue problem. Note that this ratio of the steady state does not change the magnitude of the steady state. The coincidence between two values for small $1/k$ (<0.5) means that the main flow plus a considerably large amplitude of the most unstable mode corresponds to the steady state satisfied by the nonlinear equation. Indeed we do not accept that this severely truncated system is still valid in a strongly supercritical state. In this sense this coincidence partially supports

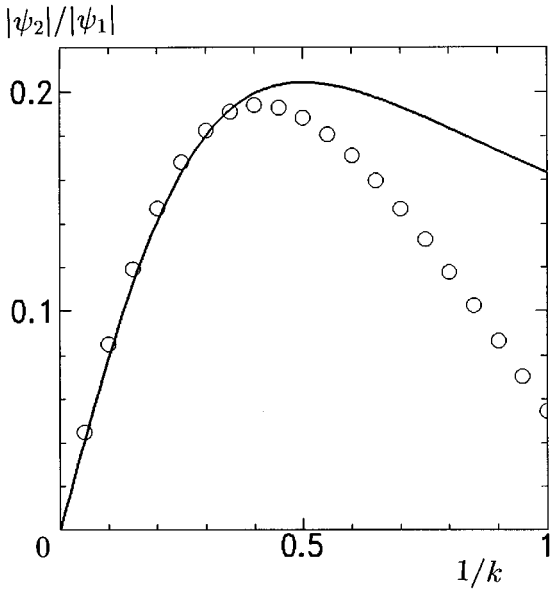

FIG. 14. The ratio of the most energy-containing mode to the main flow: $|\psi_2|/|\psi_1|$. The solid line shows the results of the steady state (the latter fixed point) in the truncated system while the open circles are obtained by the linear eigenvalue problem.

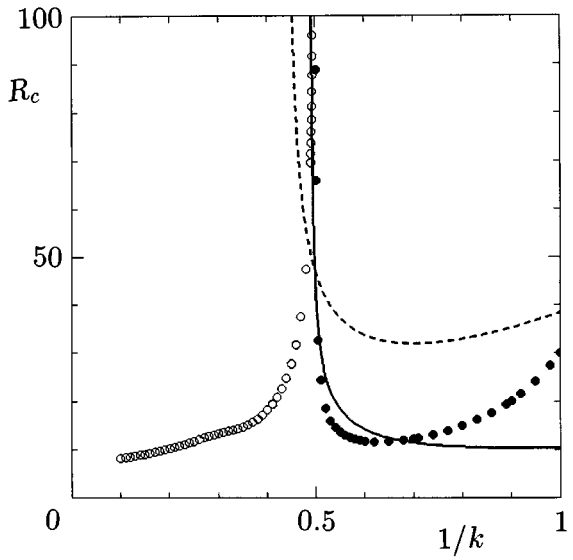

FIG. 15. The critical Reynolds number R_c in the range $0<1/k<1.2$ for $M=2$. Bold line, $c_3=0$; dashed line, $c_1c_2-c_3=0$ by the four-mode system; closed circles, the stationary mode; open circles, the oscillatory mode by the converged values of the eigenvalue problem.

the position that the streamlines of the naive superposition of the linearly unstable mode on the main flow resemble those of the laboratory experiment for $k=0.33$ in [8].

B. A pair of vortices

We apply the same principle of the selection of the components in order to obtain the minimum truncated system. The most energy-containing component in the most unstable mode is $\sin kx/2 \sin y$ of the system size. Two other components are generated through the nonlinear interaction between the main flow and this component. Hence we set

$$\psi=\psi_0(t)\sin kx\ \sin y+\psi_1(t)\sin\frac{kx}{2}\sin y+\psi_2(t)\sin\frac{kx}{2}\sin 2y + \psi_3(t)\sin\frac{3kx}{2}\sin 2y. \tag{20}$$

Substitution of Eq. (21) into the basic equation (4) gives the coupled ordinary differential equations as follows:

$$\frac{d\psi_0}{dt}=\frac{k(2k^2+3)}{8(k^2+1)}\psi_3\psi_1-\frac{9k}{8(k^2+1)}\psi_2\psi_1-\frac{k^2+1}{R}\times(\psi_0-f), \tag{21}$$

$$\frac{d\psi_1}{dt}=-\frac{9k(k^2-4)}{8(k^2+4)}\psi_0\psi_2-\frac{k(5k^2+12)}{8(k^2+4)}\psi_0\psi_3-\frac{k^2+4}{4R}\psi_1, \tag{22}$$

$$\frac{d\psi_2}{dt}=\frac{9k^3}{8(k^2+16)}\psi_0\psi_1-\frac{1}{R}\frac{k^2+16}{4}\psi_2, \tag{23}$$

$$\frac{d\psi_3}{dt}=-\frac{3k^3}{8(9k^2+16)}\psi_0\psi_1-\frac{1}{R}\frac{9k^2+16}{4}\psi_3. \tag{24}$$

Here we do not try to obtain all steady states. We only consider the linear stability of the trivial steady state:

$$\overline{\psi_{p0}}=F,$$

$$\overline{\psi_{pj}}=0 \quad (j=1-3). \tag{25}$$

Employing the linear stability analysis of the steady state we obtain the characteristic equation

$$\sigma^3+c_1\sigma^2+c_2\sigma+c_3=0, \tag{26}$$

where we do not give the explicit form of the coefficients c_j $(j=1-3)$ to save space. Applying the Rouse-Hurwitz criterion to Eq. (26), we obtain the critical Reynolds number $R_c(k)$ as shown in Fig. 15. The solid curve shows $c_3=0$ while the dashed curve shows $c_1c_2-c_3=0$. In the downside of each curve, the inequality $c_3>0$ and $c_1c_2-c_3>0$ holds, respectively. The region below both curves is stable while the other regions are unstable. The boundary $c_3=0$ indicates the exchange of stability while the boundary $c_1c_2-c_3=0$ does the overstability. It is noteworthy that the curve $c_3=0$ is very close to the critical curves by the stationary mode near $k\approx 0.5$. Hence the singular behavior around $k\approx 0.5$ is captured partially in the four-mode minimum truncated system. However, we cannot find the critical Reynolds number for $k<0.48$.

In order to reproduce the critical curve by the oscillatory mode we include five other modes generated through the nonlinear interaction between the present four modes as follows:

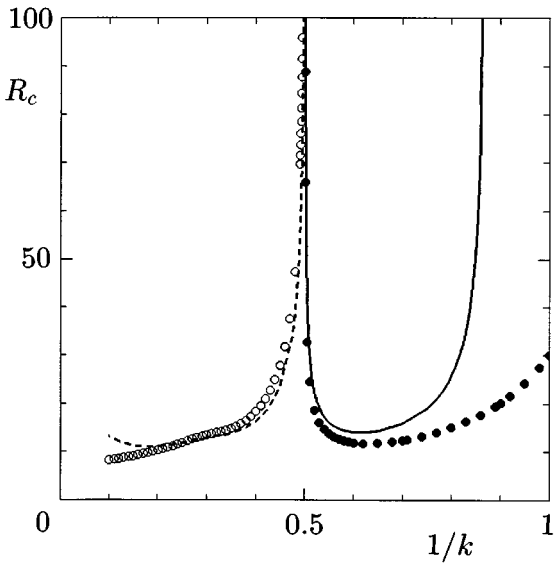

FIG. 16. The critical Reynolds number R_c in the range $0<1/k<1.2$ for $M=2$. Bold line, the stationary mode by the nine-mode system; dashed line, the oscillatory mode by the nine-mode system; closed circles, the stationary mode; open circles, the oscillatory mode by the converged values of the eigenvalue problem.

$$\psi=\psi_0(t)\sin kx\ \sin y+\psi_1(t)\sin\frac{kx}{2}\sin y+\psi_2(t)\sin\frac{kx}{2}\sin 2y+\psi_3(t)\sin\frac{3kx}{2}\sin 2y+\psi_4(t)\sin\frac{kx}{2}\sin 3y+\psi_5(t)\sin\frac{3kx}{2}\sin y+\psi_0(t)\sin\frac{3kx}{2}\sin 3y+\psi_7(t)\sin\frac{5kx}{2}\sin y+\psi_8(t)\sin\frac{5kx}{2}\sin 3y. \tag{27}$$

Substitution of Eq. (21) into the basic equation (4) gives the coupled ordinary differential equation, whose form is omitted here. The linear stability analysis is performed numerically. The results on the critical curves $R_c(k)$ are given in Fig. 16. The critical curve by the oscillatory mode is satisfactorily reproduced in addition to the curve by the stationary mode. It is remarkable that two curves are very close to the converged value of the eigenvalue problem in the region $1/k<0.6$. The singular behavior around $k\approx 0.5$ is captured in this nine-mode truncated system. However, we note that the increase of the critical Reynolds number with increasing $1/k$ is overestimated noticeably. We need to increase the truncated number of modes to reproduce this feature. Hence two types of growth of the critical Reynolds number exist: one is approximated by a few modes, the other is essentially due to many modes.

Numerical simulation of the nine-mode truncated system shows that the unstable mode to the main flow, ψ_p, grows to saturate and constitutes the secondary steady flow ψ_s for $1/k=0.6,0.7$. It is confirmed that the amplitude of the secondary flow grows as $\sqrt{R-R_c}$. Hence this bifurcation is *normal* pitchfork. The stable secondary oscillatory state is also found for $1/k=0.2,0.3$ by numerical simulation. The amplitude dependence is also found to depend on $\sqrt{R-R_c}$. Therefore this bifurcation is regarded as *normal* Hopf.

V. CONCLUDING REMARKS

We have analyzed the stability and the bifurcation of the planar rectangular cell flow, $\Psi=\sin kx\sin y$ $(0<k<\infty)$, in an infinite array of the x direction $[(-\infty,\infty)\times[0,\pi]]$ or finite M arrays ($[0,M\pi/k]\times[0,\pi]$, $M=2,3,4$) on the assumption of a *stress-free* boundary condition on the lateral walls.

The numerical results of the eigenvalue problems on the infinite array reveal that a mode representing a global circulating vortex in the whole region ($\psi\approx\sin y$) appears in the y-elongated cases ($1/k<1$), while a mode representing *quasiperiodic* arrays of counter-rotating vortices appears in the x-elongated cases ($1/k>1$) at large critical Reynolds number.

We clarify that the type of bifurcation is normal pitchfork for y-elongated cases by the truncated system of three modes. The three-mode truncated system is essentially the same as the three-wave resonance with constant forcing and damping [15]. The instability mechanism is decay-type according to the terminology of the plasma physics. Hence the oscillatory unstable mode cannot appear in this case.

We do not intend to discuss a quantitative value of saturated amplitude by the severely truncated system. Nevertheless, it is appropriate to discuss the effect of the bottom friction and the truncation level on the nonlinear saturation. Dauxois *et al.* [16] have shown numerically that the nonlinear saturation should depend on the bottom friction strongly in the case of the Stuart vortices. In their study the bottom friction makes the equilibrium amplitude small; it may be regarded as a stabilizing effect. Hence the equilibrium amplitude would be smaller in our case if we included the bottom friction. We have confirmed that the qualitative nature of the bifurcation (normal) is unchanged by the increase of the truncation level in some cases.

One peculiar feature of the x-elongated vortices is the large critical Reynolds number, e.g., $R_c>50$ for $1/k=1.1$. The qualitative interpretation is as follows: The relative length of the adjacent side, π/k, becomes smaller as the vortices becomes x-elongated ($1/k$ becomes larger). Hence the interaction between corotating vortices may be *weak*; the vortex merging is not likely to occur.

Another unique feature of the x-elongated vortices is the appearance of the *quasiperiodic* structure of the mode. General theory on instabilities of one-dimensional cellular patterns has been proposed by Coullet and Iooss [17]. There they present several types of coupled system of amplitude and phase based on the symmetry argument and the Taylor expansion. Our finding belongs to the category (A-3) in their paper. They mention that no experimental evidence of this case is reported so far. However, it should be noted that their analysis cannot be applied to our case. The reason is as follows: They assume a neutral spatial phase mode ϕ owing to the translational invariance of a homogeneous system. In our system the external forcing breaks this symmetry; no neutral phase can exist. In the atmosphere the x-elongated convec-

tion is often observed. It is of great interest to clarify whether the spontaneous formation of the quasiperiodic structure is observed or not in the secondary bifurcation of this case, though the three-dimensional effect may play an essential role in this case.

In a pair of planar counter-rotating vortices, the global circulating stationary mode, which is similar to the infinite array case, appears for $1/k>0.5$ while another oscillatory mode appears for $1/k<0.5$. At the point $k_0\approx 0.5$ between the regions of the two modes the critical Reynolds number takes an extreme large value. Based on the analysis of the four-mode truncated system the singular behavior of the critical Reynolds number of the stationary mode is reproduced qualitatively. However, the critical Reynolds number by the oscillatory mode for small $1/k$ ($1/k<0.45$) is not found. Hence the oscillatory nature of the mode is not obtained by the minimum truncated system. The results on the next stage of the truncated system (nine-mode system) are similar to those of the numerical eigenvalue problems including the oscillatory instability and the singular behavior. Hence the singular behavior of the critical Reynolds number is captured by a low-dimensional dynamical system. However, the apparent discrepancy around $1/k>0.8$ is found. In this region a large number of the modes are necessary to obtain a reliable critical Reynolds number in contrast with the region $1/k\approx 0.5$. Based on this truncated system, we clarify that both pitchfork and Hopf bifurcations are normal.

A global circulating mode is essentially due to the existence of the lateral walls because the total angular momentum is conserved in an unbounded region without walls even in the viscosity-dominant flow. Apparently the growth of the global circulating mode destroys the angular momentum conservation because the initial state has no total angular momentum. In the rapidly diverging channel a pair of elongated vortices attached to the walls, which is symmetric in the centerline of the channel, is observed at the relatively low Reynolds number. Beyond the critical Reynolds number one of the vortices becomes larger while the other becomes smaller, which is similar to our case in Fig. 11. We expect that this symmetry-breaking transition is essentially the same as ours, though the main flow along the channel exists in this case. In this sense the merging of the counter-rotating vortices in confined system is universal. Our results suggest that a local oscillation may be observed if a pair of very elongated vortices appears in the channel.

One severe restriction of our study is to apply the artificial stress-free boundary condition. However, the previous work shows that the structure of the mode explains the pattern observed in the experiment by Tabeling *et al.* The work of Nakamura [18], who applies the viscous lateral boundary in the direct numerical simulation of the arrays of the planar vortices, shows that the viscous boundary condition should be used to obtain the correct value of the critical Reynolds number for the primary bifurcation. At the present stage we speculate that the pattern of our results is not changed appreciably while our critical Reynolds number is changed significantly if we apply the viscous boundary condition. The numerical treatment of the eigenvalue problem with the viscous boundary condition is now in progress. The detail of the results will be reported elsewhere.

ACKNOWLEDGMENT

We acknowledge Professor M. Tajiri for his encouragement throughout this work.

[1] A. C. Newell, T. Passot, and J. Lega, Annu. Rev. Fluid Mech. **25**, 399 (1993).
[2] M. C. Cross and P. C. Hohenberg, Rev. Mod. Phys. **65**, 851 (1993).
[3] P. Manneville, *Dissipative Structures and Weak Turbulence* (Academic, San Diego, 1990).
[4] N. F. Bondarenko, M. Z. Gak, and F. V. Dolzhanskii, Izv. Atmos. Oceanic Phys. **15**, 711 (1979); F. V. Dolzhanskii, V. A. Krymov, and D. Yu. Manin, Usp. Fiz. Nauk **160**, 1 (1990) [Sov. Phys. Usp. **33**, 495 (1990)]; F. V. Dolzhanskii, V. A. Krymov, and D. Yu. Manin, J. Fluid Mech. **241**, 705 (1992).
[5] J. Sommeria, J. Fluid Mech. **170**, 139 (1986).
[6] P. Tabeling, B. Perrin, and S. Fauve, Europhys. Lett. **3**, 459 (1987); P. Tabeling, O. Cardoso, and B. Perrin, J. Fluid Mech. **213**, 511 (1990).
[7] H. Honji, J. Phys. Soc. Jpn. **60**, 1161 (1991); H. Honji and H. Haraguchi, *ibid.* **64**, 2274 (1995).
[8] K. Gotoh, Y. Murakami, and N. Matsuda, Phys. Fluids **7**, 302 (1995).
[9] S. D. Danilov, F. V. Dolzhanskii, and D. Yu. Manin, Ann. Geophys. **11**, 104 (1993).
[10] A. Thess, Phys. Fluids A **4**, 1396 (1992).
[11] H. Fukuta and Y. Murakami, J. Phys. Soc. Jpn. **65**, 1655 (1996).
[12] I. J. Sobey and P. G. Drazin, J. Fluid Mech. **171**, 263 (1986).
[13] U. Miura, J. Atmos. Sci. **43**, 26 (1986).
[14] A. M. Batchayev, Izv. Atmos. Oceanic Phys. **25**, 316 (1989); A. M. Oboukhov, F. V. Dolzhanskii, and A. M. Batchaev, in *Topological Fluid Mechanics*, edited by H. K. Moffatt and A. Tsinober (Cambridge University Press, Cambridge, 1990), pp. 304–314.
[15] A. D. McEvan, D. W. Mander, and R. K. Smith, J. Fluid Mech. **55**, 589 (1972); Y. Murakami, Wave Motion **9**, 393 (1987).
[16] T. Dauxois, S. Fauve, and L. Tuckerman, Phys. Fluids **8**, 487 (1996).
[17] P. Coullet and G. Iooss, Phys. Rev. Lett. **64**, 866 (1990).
[18] Y. Nakamura, J. Phys. Soc. Jpn. **65**, 1666 (1996).